STM JOURNALS

Journal of
Polymer & Composites

ISSN: 2321-2810 (Online)
ISSN: 2321-8525 (Print)
Volume 11, Special Issue 2, 2023
DOI (Journal): 10.37591/JoPC

http://engineeringjournals.stmjournals.in/index.php/JoPC/index

Research JoPC

Preparing Chitosan Hybrid Nanocomposites by Novel Additives for Wound Healing

Ishraq Abboodi Fadhil[1,*], Balqees Mohammed Dheyaa Aldabbagh[2], Wijdan Thamir Mahdi[3]

Abstract

Biomaterials made from chitosan have been discovered to be particularly unique marine polysaccharides (or polycarbohydrates) with a wide range of physico-chemical and biological characteristics suitable for biomedicine field. Due to net positive charge of chitosan, it is essentially capable of chemically binding with negatively charged surfaces A biodegradable blend of chitosan nanoparticles (CHT), poly vinyl alcohol (PVA) and polyethylene glycol (PEG) hybridized with metal oxides nanopowders were prepared and used for wound healing application. The exploited oxides were titanium dioxide (TiO_2), zinc oxide (ZnO), and magnesium oxide (MgO). Scanning electron microscopy (SEM), differential scanning calorimetry (DSC), thermogravimetric analysis (TGA), and in vivo study by applying the final gels on the injured skins were used to characterize the morphology, thermal, and biological properties of hybrids. The in vivo animal tests were employed to confirm the biocompatibility of the nanocomposites as wound healers. The hybrid's ability for wound healing has been improved by combining PVA, PEG, and CHT along with the proper concentrations of TiO_2, ZnO, and MgO. The aim of this work was to create an attractive product for wound healing could be used for human health care. Consequently, dual/triple-hybrid systems have been adopted by integrating TiO_2/MgO, TiO_2/ZnO, MgO/ZnO, and TiO_2/MgO/ZnO nanocomposites. Eventually, the wound contraction was accelerated by treating the injured skin with a ternary-hybrid system within a period of less than a week with no toxicity up to concentration of 100 µg/mL on WRL-68 cell line. All the parameters observed (presence of necrotic tissue, clotting and crust, re-epithelialization and granulation tissue growth) were affected; suggesting that chitosan and the metals oxides nanoparticles have a substantial efficiency in tissue regeneration. This is an indication to collagen maturation progress. Based on the results, the previously mentioned hybrid will be a promising nontoxic biomaterial for wound treatment application. The in vivo model revealed that the novel composite of CHT/PVA/PEG blend hybridized with the three different types of the suggested metals oxides have superior curing effect as compared to Fucidin ointment.

Keywords: Chitosan blend, hybrid, nanocomposites, wound healing, biocompatibility, biodegradability

***Author for Correspondence**
Ishraq Abboodi Fadhil
E-mail: iishraq.obaid@qu.edu.iq

[1]Lecturer, Dr, University of Al-Qadisiyah/College of The Education/Department of Physics, Iraq
[2]Professor, Dr, University of Technology/Department of Applied Science/Materials Science, Iraq
[3]Professor, Dr, University of Al-Qadisiyah/College of Science/Department of Biology, Iraq

Received Date: December 08, 2022
Accepted Date: January 31, 2023
Published Date: June 19, 2023

Citation: Ishraq Abboodi Fadhil, Balqees Mohammed Dheyaa Aldabbagh, Wijdan Thamir Mahdi. Preparing Chitosan Hybrid Nanocomposites by Novel Additives for Wound Healing. Journal of Polymer & Composites. 2023; 11(Special Issue 2): S9–S23.

INTRODUCTION

Because skin is the first and largest human body organ to be wounded, it has high self-healing potential. The natural wound healing process may be inadequate or insufficient in the event of severe lesions or extensive surface loss, resulting in harmful and painful situations that require repair adjuvants and tissue replacements. Biodegradable polymers, both synthetic and biologic origin, are gaining increased importance for their high biocompatibility, biodegradation, and bioactive

properties, such as antimicrobial, immunomodulatory, cell proliferative, and angiogenic properties, in addition to conventional wound care options [1].

The ability of multicellular organisms to repair wounds is crucial for their survival. The wound healing process is a series of coordinated reactions to tissue damage which leads to tissue contraction, closure, and restoration. Hemostasis, inflammation, proliferation, and maturation or remodeling are the four continuous stages of wound healing. Epithelialization (the migration and division of keratinocytes from the lower layers of the skin), contraction, and connective tissue (matrix) deposition are all involved in wound healing [2].

Chitin and chitosan are attractive materials for biomedical and pharmaceutical applications because they offer beneficial features, such as non-toxicity, biodegradability, and biocompatibility [3]. Due to their reactive hydroxy and amino groups, high charge density, extensive hydrogen-bonding capabilities, and the single chemical structure, these materials frequently exhibit a wide range of properties. The combination of various physicochemical and biological characteristics allows for a wide range of biomedical applications [4]. The aim of polymeric hybrid reinforcement is to achieve considerable and desired characteristics by using multiple types of reinforcements [5]. They may collect and store a substantial amount of wound exudates in the interstitial regions of their networks, allowing them to maintain appropriate local wetness [6].

It is commonly believed that an effective wound healing agent should have the following characteristics: It should offer an ideal microenvironment rich in cytokines, enzymes, white cells, and growth factors that are favorable to the continuous tissue recovery process. It must also prevent the bacterial infection, limit excessive fluid loss, provide a moist healing environment, and be biocompatible. In addition, it must stick adequately to the wound surface and be easy to apply and remove to enhance patient safety and satisfaction [7].

Hydrogels are organic cross-linked hydrophilic polymers with a water basis of 80% to 90%. These gels come in two types: free-flowing amorphous and fixed flexible sheets. They can absorb a little amount of fluid via swelling, but they may also contribute moisture to a dry wound, allowing for autolytic debridement and the maintenance of a moist, thermally insulated wound environment. They have also been proven to stimulate granulation and epithelialization, as well as lessen wound bed temperatures by up to 5°C. They are gas and water permeable, and they have been shown to be a less effective bacterial barrier than occlusive dressings [8].

The novelty of our work lies in using chitosan hybrid nanocomposite materials as a gel form applied to the wound surface instead of forming adhesive films or a fiber web. To the best of our knowledge, no study has been performed that is similar to the prepared hybrid biomaterials with the addition of ternary mixed oxides as wound healing and anticancer product. It took less than a week for the wound scar to completely vanish.

EXPERIMENTAL METHOD

Materials

Chitosan nanopowder, produced by Micxy Chemical Co. with a degree of deacetylation (DD) of 95.7% and about 80 nm particle size, was used. Polyvinyl alcohol (PVA; average molecular weight 67000 g mol^{-1}) and polyethylene glycol (PEG; average molecular weight 3500 g mol^{-1}) were also utilized as plasticizer polymers. Rutile TiO_2, ZnO, and MgO nanoparticles (<50 nm) with high purity >99% were bought from a Chinese resource. Acetic acid glacial (extra pure/molecular weight 60 g mol^{-1}) produced by Tomas Baker/India was also used as a solvent with chitosan. Distilled water was required as a solvent and to clean the used tools.

Preparation of the Main Polymeric Solutions

Separate steps were followed to prepare chitosan (CHT), PVA and PEG solutions. First, a 1.5 g of chitosan nanopowder was dissolved in a 100 mL distilled water along with the addition of 2 mL acetic

acid (2% concentration) that is a good solvent for chitosan. The mixture was well stirred at room temperature and moderate speed for about 30 min by using a magnetic stirrer. A clear and homogeneous solution was optically seen and kept away into a sealed container. Five grams of each PVA and PEG polymers were dissolved in a 100 ml of distilled water, separately. To produce a 5% concentration of each agent; the PVA solution was prepared at 80℃ with 15 min stirring, whereas the PEG solution was mixed using a sonicator bath at room temperature for 5 min and then saved into sealed containers, individually.

Hydrogel Synthesis

In recent decades, metallic nanomaterials have interestingly attracted researchers and rapidly revolutionized many scientific fields [9–12]. In this study, CHT/PVA/PEG were blended with the aforementioned metal oxide nanoparticles to form a hybrid so as to investigate their potential as wound healing products. A sensitive electronic balance was used to measure various amounts of each type of metal oxides (0.04, 0.06, and 0.08 g). Firstly, we put 0.04 g of MgO in a plastic beaker and then added 1 mL of the PVA solution shaking well with a magnetic stirrer for 1 min. After that, 1 mL of PEG solution was poured to the mixture with continuous stirring for 1 min. When a clear white blend was observed, 5 mL of the previously prepared chitosan was gradually added (drop by drop) by a burette and the final product was left under continuous stirring for 30 min. The exact same steps were managed for two other amounts (0.06 and 0.08 g) of MgO. Similar steps were followed to form ZnO/CHT/PVA/PEG hydrogel with three different weights of ZnO, as stated before. However, preparing TiO_2 nanocomposite was slightly changed by adding few drops of NaOH with strong base to TiO_2 nanopowder as a solvent. To remove any NaOH residue left over from the filter papers, the final blend was thoroughly washed with distilled water. Subsequently, three ratios of TiO_2 hydrogel (0.04, 0.06, and 0.08 g) were produced. Field emission scanning electron microscopy (FE-SEM), differential scanning calorimetry (DSC), thermogravimetric analysis (TGA), in vivo, and histological studies were performed in order to create a novel biomaterial gel that is useful for wound healing, as shown in Figure 1.

Figure 1. The final appearance of the mixed gels which used as an innovated wound healing product.

Experimental Animals

The present study was conducted in the animal house of the College of Veterinary Medicine, University of AL-Qadisiyah during the period from September 20, 2021 to November 20, 2021.

Twenty mature male mice (aged 75 ± 5 days and weighing 30 ± 3 g) were used in three experimental periods of the present study. Before beginning the experiment, male mice were allowed to acclimatize to the animal house environment. Animals were housed in polypropylene cages inside a

well-ventilated room. Each cage consists of not more than two mice. Male mice were fed on the standard chow and drinking water ad libitum throughout the experiment. Room temperature was maintained at 23°C ± 2ºC. Throughout the experimental periods, the light/dark cycle had the light ON for 12 hours from 06:00 a.m. and OFF at 06:00 p.m.

Operation Steps

Firstly, mice were brought to the workplace and anesthetized by intraperitoneal injection of 0.3 mL of ketamine and 0.1 mL of xylazin. After that, the back hair was shaved at a distance of 1.5 cm longitudinally, while the area was well sterilized. Mice in each group were anesthetized, and two paravertebral-long incisions of approximately 1.5 cm were made through the skin and cutaneous muscles at a distance of about 1.0 cm from the midline on each side of the depilated back of the mice.

Experimental Design

After the incision of the skin area, 20 mature male mice were randomly assigned into 10 equal groups (2 in each group), then treated for three periods (7 days), as presented in Table 1.

Table 1. Experimental design for 10 tested groups

Sample no.	Treatment way	Sample no.	Treatment way
1	Control/without treatment	6	Treatment with 0.04 g MgO nano-hybrid
2	Treatment with Fucidin ointment	7	Treatment with the mix of 4 and 5
3	Treatment with CHT/PVA/PEG blend	8	Treatment with the mix of 4 and 6
4	Treatment with 0.04 g TiO_2 nano-hybrid	9	Treatment with the mix of 5 and 6
5	Treatment with 0.06 g ZnO nano-hybrid	10	Treatment with the mix of 4, 5, and6

CHT, chitosan; PEG, polyethylene glycol; PVA, polyvinyl alcohol.

RESULTS AND DISCUSSION

Fourier Transform Infrared (FT-IR) Spectroscopy

The FT-IR spectra were managed within the range of 500 and 4000 cm^{-1}, but the major fingerprints of the tested samples were between 1000 and 3700 cm^{-1}, as shown in Figure 2. Five samples were characterized by infrared spectrum which were labeled as the control (CHT/PVA/PEG) blend, ZMT (the mixture of tertiary metal oxides hybridized with the control), MT (the mixture of magnesium and titanium oxides hybridized with the control), ZT (the mixture of zinc and titanium oxides with control), ZM (the binary mixture of zinc and magnesium oxides hybridized with the control). The broad distinctive peak in the range 3100 to 3750 cm^{-1} related to the stretching vibration of –OH, –CH, and $–NH_2$ bonds. From previous work [13], the reference crystallization band of pure chitosan at 1078 cm^{-1} did not appear in the blend status for the control sample, which is probably an indication that the crystallinity of chitosan has been disrupted by intermolecular interaction between PVA/PEG and CHT [14]. Furthermore, it could be elucidated that the process of mixing two or more polymers may motivate obvious changes in the main spectral peaks, owing to the physical blend reflection and chemical interactions that occur [15, 16]. The characteristic band at 1095 cm^{-1} was attributed to the C-O bending vibration for PVA and PEG blended with CHT (control) [17]. A slightly sharp band at 1610 cm^{-1} refers to the carboxymethyl group (–COO) of chitosan on the blend curve [18]. Additionally, the region between 2890 and 2920 cm^{-1} represents $–CH_2$ groups asymmetric and symmetric stretch, respectively [19].

The remaining four spectra in Figure 2 display the hybrids of chitosan/nanometal oxides as binary and tertiary mixtures. From the bottom to up: CHT blend/(ZnO, MgO, TiO_2) was grouped as ZMT, CHT blend/(MgO, TiO_2) was categorized as MT, CHT blend/(ZnO, TiO_2) was labelled as ZT, and finally, CHT blend/(ZnO, MgO) was identified as ZM. The characteristic bands for the all hybrids were acceptably similar, nevertheless, notable differences in peaks' width and intensities could be observed in ZT and ZM curves, which could be responsible for either the conditions of composites' preparation or test procedure. It has been stated that ($–NH_2$ and –OH) functional groups in the

chitosan backbone are attributed to the interaction of constituents via a coordination bond between the presented nitrogen in the (–NH2) group with TiO_2, which is represented at wave numbers of about 3450 cm^{-1} and 1537 cm^{-1} in ZMT, MT, and ZT patterns. Predominantly, an active site for the adsorption of inorganic and/or organic compounds is considered to have occurred [20, 21]. Saravanan et al. [22] pointed out that the stretching bands at 3350 cm^{-1} and 2921 cm^{-1} were attributed to the –NH_2, –OH, and C–O groups bonding with the nano-TiO_2, allowing the creation of a hybrid composite (ZMT, MT, and ZT) by electrostatic interactions of N–H–O–Ti bonds. Similarly, the –NH_2 functional group was assigned to the stretching bands of C=O near 1640 cm^{-1}, N–H bending around 1530 cm^{-1}, and 1410 cm^{-1} for C–H bending [22], while the absorption band at about 1029 cm^{-1} indicates that chitosan and nanometal oxides (Z, M, and T) chemically interacted by bonding with —O—C— rather than being just a physical saturation of metal oxides nanopowders into the polymeric matrix [23]. The Zn–O, Mg–O, and Ti–O bonds are responsible for the region between 620 and 550 cm^{-1} bands. Practically, the integration of a ternary and binary systems (ZMT, MT, ZT, and ZM) did not modify the characteristic structure of chitosan [24]. Anaya-Esparza et al. [25] proposed that the functionalization of chitosan doped with TiO_2:Cu did not change the typical structure of chitosan.

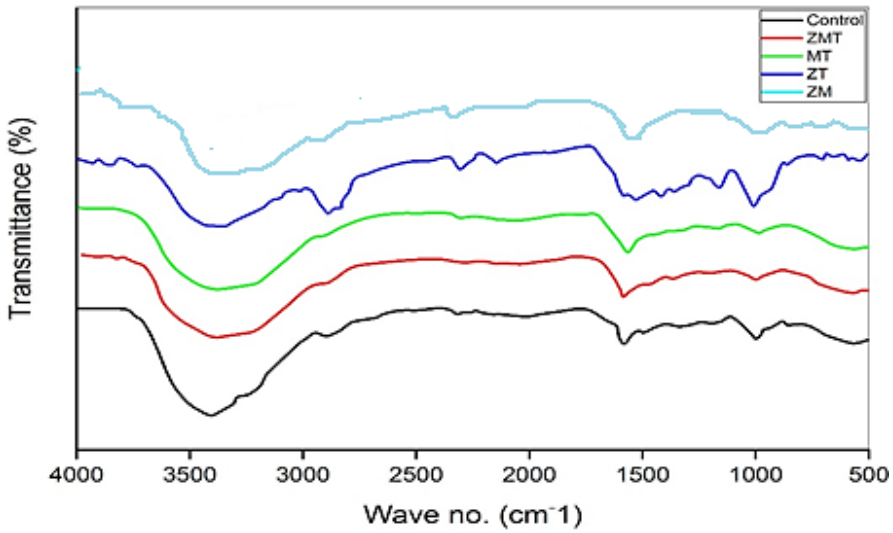

Figure 2. Fourier transform infrared (FT-IR) patterns for control (CHT/PVA/PEG) blend, ZMT (the mixture of tertiary metal oxides hybridized with control), MT (the mixture of magnesium and titanium oxides hybridized with control), ZT (the mixture of zinc and titanium oxides with control), ZM (the binary mixture of zinc and magnesium oxides hybridized with control).

Swelling

The degree of swelling, also known as a degree of expansion, is one of the most important properties of a hydrogel. This parameter denotes an essential criterion of polysaccharide-based resources for biomedical purposes, especially for advanced therapeutic materials [26]. Swollen samples change their weights as a result of hydrogel behavior of the samples, that is, the entry of water molecules into the polymeric network due to the hydrophilic balance of the system. Figure 3 illustrates a typical swelling behavior for the ZnO (0.06 g), MgO (0.04 g), TiO_2 (0.04 g), MT, ZT, ZM, and ZMT that were hybridized with CHT blend. The findings showed that the swelling degree had changed as the kinds of additives were altered. All of the tested blends have continuously shown swells at a proportional rate for up to 5 hours with different percentages of swelling for each hybrid. This behavior can be explained by the water solubility of carboxymethyl molecules on the polymeric chains of the prepared hydrogels [19]. After 5 hours, the swelling rate steadily increased until the end of the selected period (48 hours), tending to be a constant rate for almost curves. The results endorsed that adequately cross-linked networks formed by the intermolecular reactions on the polymer chain had occurred. The hydrogel's flexibility and number of hydrophilic groups were consequently altered, which were related to the hydrogel mechanism [27]. To sum up, the swelling behavior is significantly

influenced by the content of added nanocomposite materials in the CHT blend, even though it is a macroscopic effect that results from the overall combined contribution of micro and nanostructures of the chemically modified network of the polymeric hybrid system [28–31]. The reason may be attributed to the absorptive properties of produced hybrids and the reinforcement of nano metal oxides, which would increase the surface to volume ratio [32] and boost the matrix density of these hybrids (binary and ternary mixtures) [33, 34]. Gels with a swelling degree at around 50% were considered as suitable curative materials for wound healing.

Table 2 explains the data of the swelling experiment for examined hybrids. The period interval of the test was between 0 and 48 hours. The swelling degree (*SD*) was computed according to Equation (1) in terms of the absorbed water amounts relative to the initial quantity of a tested sample and extracted as a percentage form, where (W_w) is the wet mass and (W_0) is the initial amount, as follows

$$SD(\%) = \left[(Ww - W0)/(Ww)\right] \times 100 \quad (1)$$

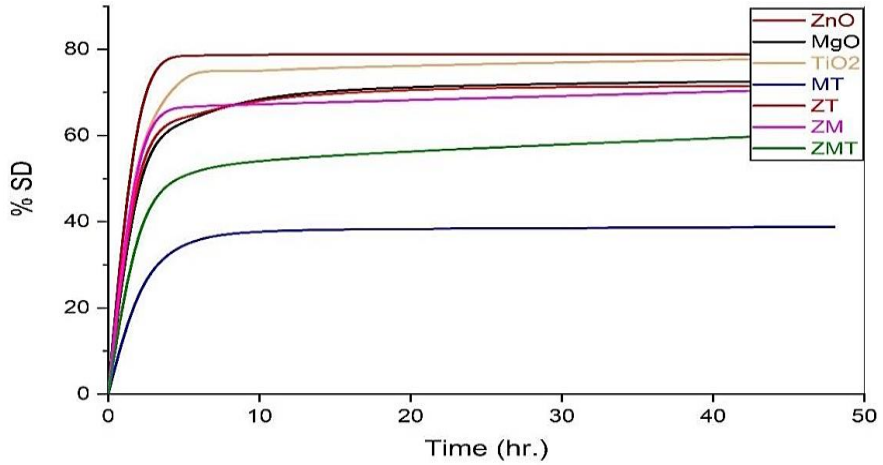

Figure 3. The swelling degree of chitosan blends functionalized with ZnO, MgO, TiO_2, MT, ZT, ZM, and ZMT nanopowders.

Table 2. Presents the swelling data for prepared hybrids (ZnO, MgO, TiO_2, MT, ZT, ZM, and ZMT nanopowders).

Time (hours)	ZnO %	MgO %	TiO_2 %	MT %	ZT %	ZM %	ZMT %
0	0	0	0	0	0	0	0
2	78.2	58.3	53.5	27	61.4	65.7	44.2
5	78.5	63.3	73	36.2	64	66.7	51.9
10	78.8	70	75	38.2	69.2	67.3	54.5
24	78.8	71.9	76.5	38.4	71.4	68.6	57.1
48	78.8	72.7	78	38.8	71.4	70.9	60.5

Field Emission Scanning Electron Microscopy (FE-SEM) Analysis

SEM is a valuable tool to evaluate the scaffold characteristics such as structures, shapes, sizes and other surface morphology of the prepared product. Figure 4 shows the FE-SEM micrographs of CHT/PVA/PEG blends loaded with 0.04 g TiO_2, 0.06 g ZnO, 0.04 g MgO, TM, ZM, ZT, and ZMT nanopowders with two magnification powers of 1 μm and 200 nm.

As can be noticed in Figure 4a–c, the CHT hybrids revealed homogeneous and reasonably smooth surfaces due to appropriate compatibility and encapsulation ability of CHT/PVA/PEG polymers with the added metal oxide nanoparticles. However, binary and tertiary hybrids (Figure 4d–f) displayed

extremely various surface morphology owing to the presence of two or three kinds of compounds that restively defer in their interactions with each other and with the polymeric groups of CHT blend. Generally, all the prepared gels exhibited obvious nanostructures represented by nanoparticles, nano-cracks, nano rods, nano layers, and nano bars/rods. The existence of TiO_2, either alone or combined with ZnO, has produced gels with structures of nano bars/rods, as shown in Figure 4a, f, and g.

This study has focused on the CHT/hybrid of mixed-three-metal oxides gel that produced the best results in skin regeneration (Figure 4g). The behavior of nano bars/rods in the examined product may explain the high efficiency of the prepared gel in rebuilding the injured skin by assembling bridge-like between the two sides of the incision region. Furthermore, preparing chitosan nanocomposite as nanofiber structures by hydrogel technique is unique among other studies and fabrication techniques.

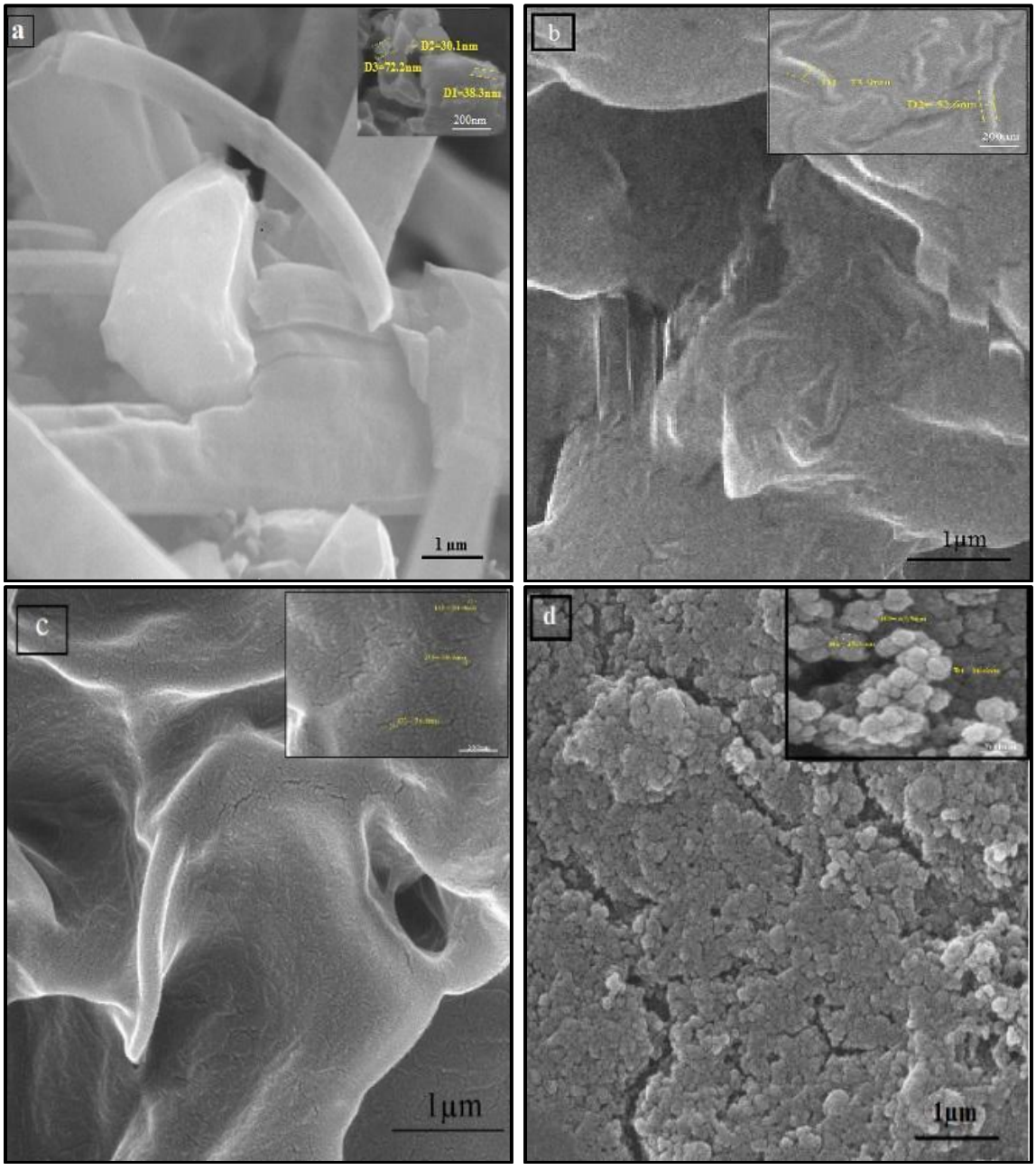

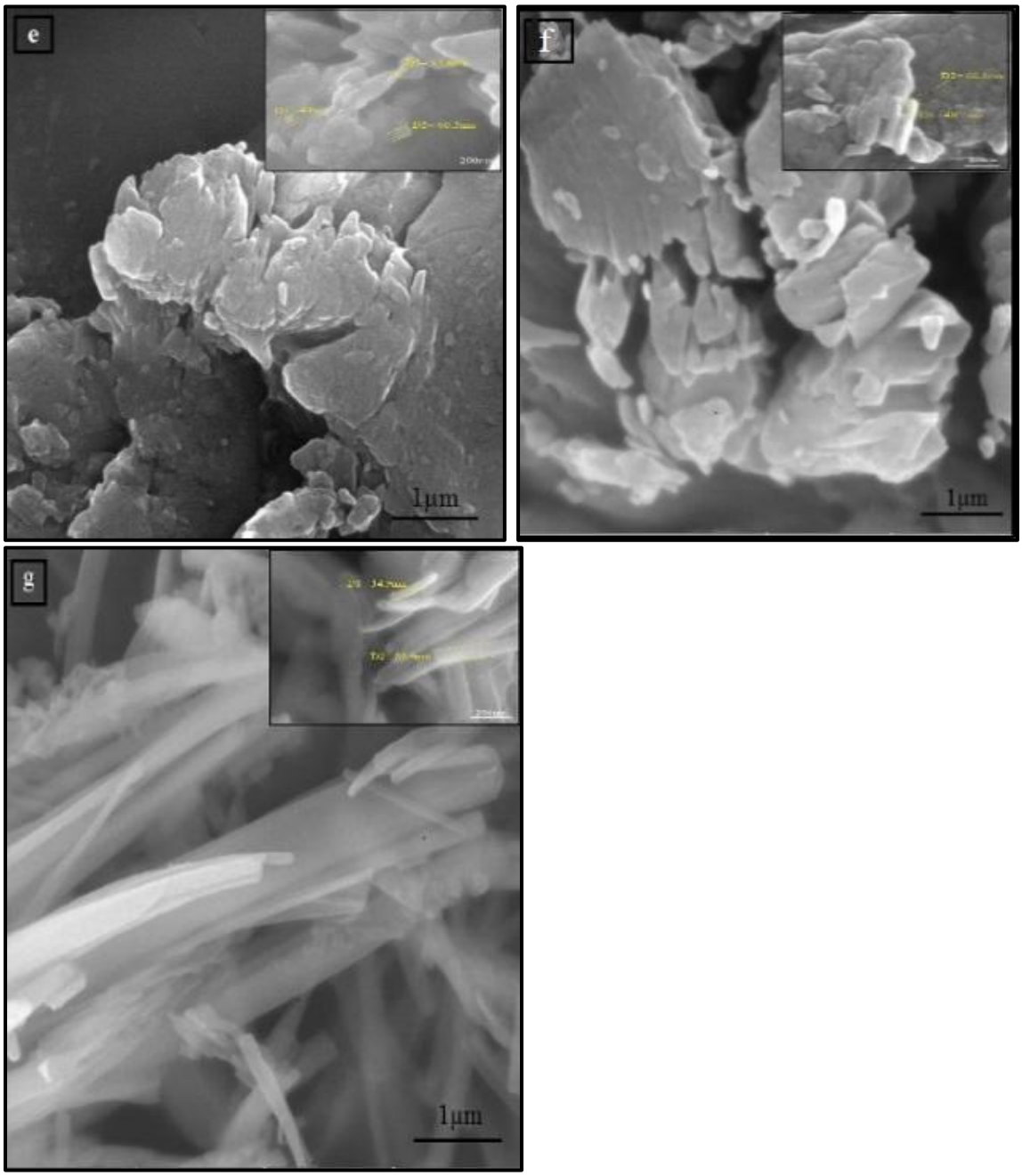

Figure 4. Field emission scanning electron micrographs of the final gel composed from CHT/PVA/PEG blend loaded with a, b, c (0.04 g TiO_2, 0.04 g MgO, 0.06 g ZnO), and d, e, f, g representing mixtures of TM, ZM, ZT, and ZMT, respectively with two magnification powers of 1 µm and 200 nm.

Differential Scanning Calorimetry Thermogravimetric Analysis (DSC-TGA)

Figure 5 shows the DSC-TGA analyses that were carried out via a Universal V4.5 A instrument by applying ramp method. Approximately 1 to 5 mg of provided mixtures were cured in the range of 25°C to 800°C with a heating rate of 20ºC/min in air.

The first endotherm peaks of CHT hybrid gels can be observed in a temperature range of 91°C to 190°C, which relates to water evaporation included within the chemical structure of the final products, and this range variation of temperature corresponds to concentration function of implanted metal

oxide nanoparticles. In other words, a free movement of water molecules between the chitosan backbones required high temperature to achieve the evaporation point [35]. It has been proposed that the thermal stability of biopolymer, particularly of CHT-based nanocomposites, is enlarged due to the combination with TiO_2 nanoparticles, which could be associated with its ability to trigger chemical interactions in the hydroxyl and amine groups held to the chitosan structure. Accordingly, most of the water molecules can perform as a plasticizer agent in CHT hybrids and have the ability to bond with –OH groups of chitosan chains, forming a wide range of hydrogen bonds, therefore needing abundant temperature to detach them. As reported by Jbeli et al. [36], the utilization of TiO_2 with ZnS can enhance the thermal strength of CHT-based films as compared to the films of only CHT-TiO_2, because of the synergistic effect between the two inorganic metals. Another study has declared that the integration of ZnO and MgO with TiO_2 nanoparticles and then added to the CHT-based films could boost the degradation temperature of the system [25].

The DSC curves in Figures 5 and 6 (ZMT) show that the thermal stability of the prepared gel is up to 433°C before decomposition, which may be due to the stronger interaction of CHT with the embedded metal oxide nanoparticles. It is known that chitosan is a semi-crystalline polymer due to its strong intramolecular hydrogen bonds on the backbone, and it also has a rigid amorphous phase because of its heterocyclic groups. The prepared gel reveals a unity hybrid system because the miscible CHT hybrid gel typically has one melting point.

The apparent weight loss within the range of 91°C to 500°C corresponds to consequent degradation and components' decomposition. The total weight losses were between 52% and 81%, as displayed in Figure 6. The ultimate end points of nanocomposite decomposition have fluctuated into the range of about 486°C to 670°C, which may be related to the synergistic effect of the employed metal oxides and their individual or collective interactions with CHT/PVA/PEG blends.

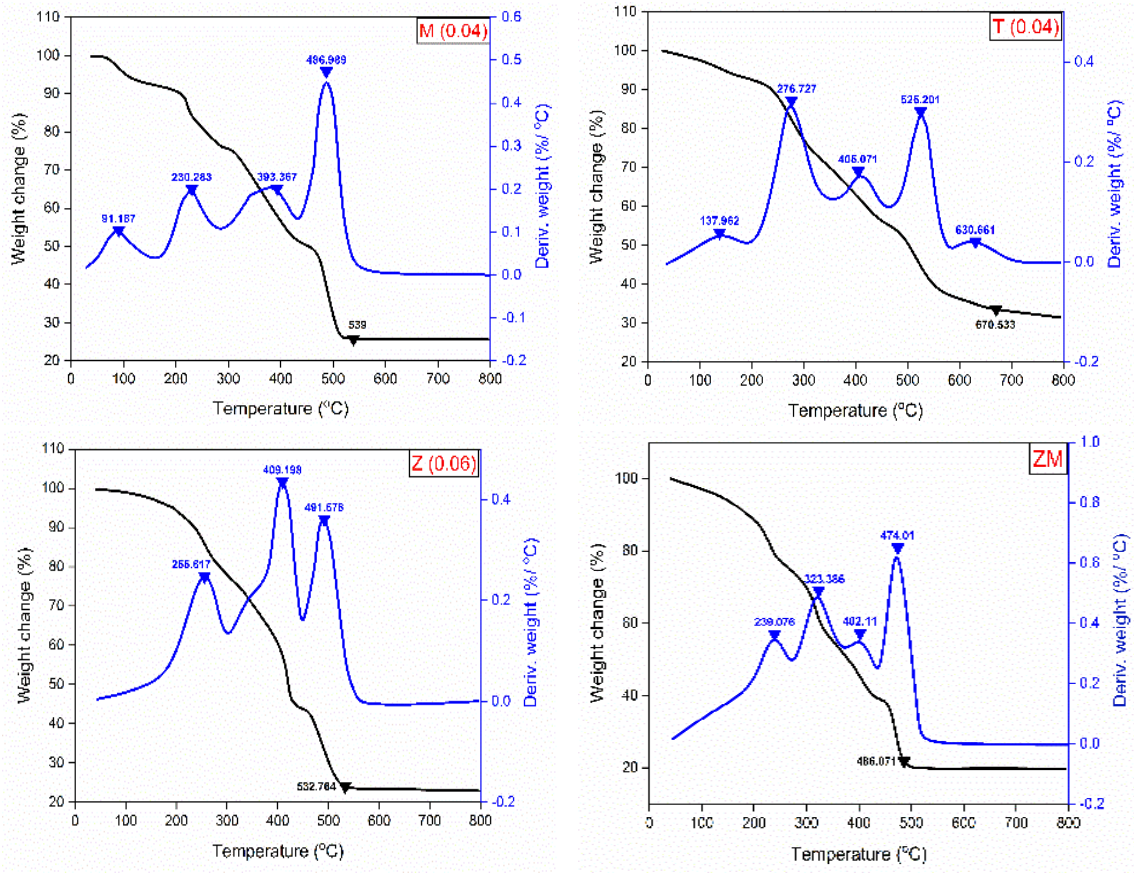

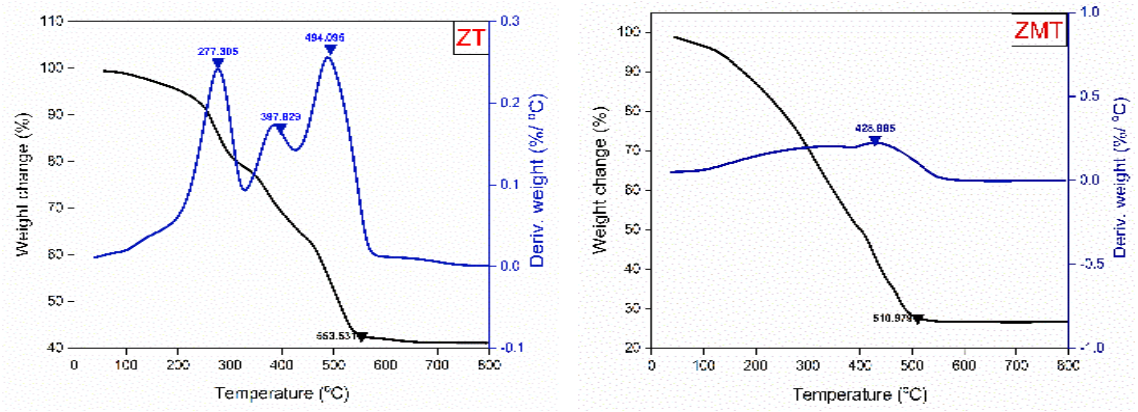

Figure 5. Differential scanning calorimetry–thermogravimetric analysis (DSC-TGA) of chitosan hybrid gels with 0.04 g MgO, 0.04 g TiO_2, 0.06 g ZnO, ZM, TM, ZT, and ZMT nanopowders.

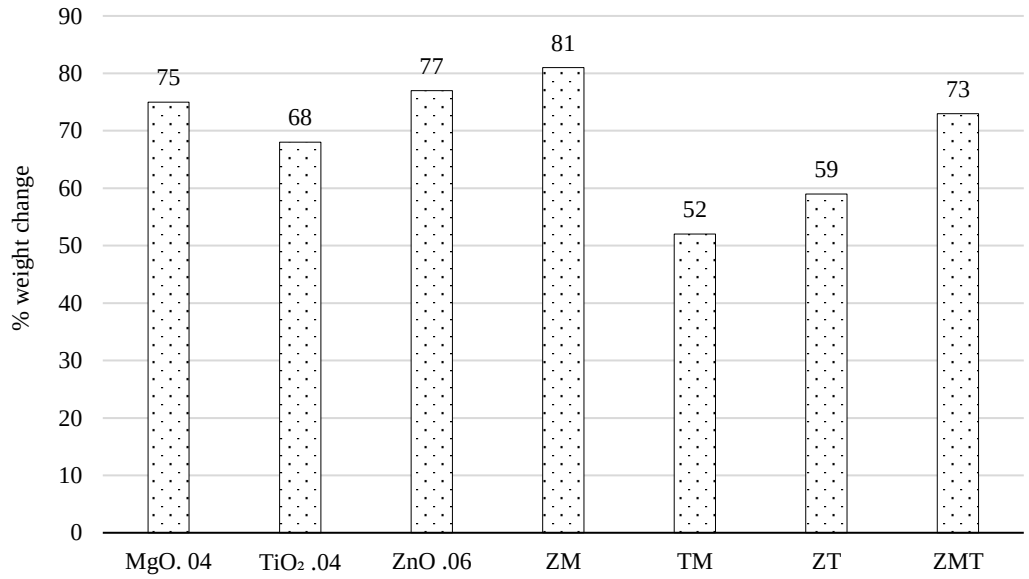

Figure 6. Column chart shows the fluctuation of percent weight change as a function of hybrids' components and their weights.

Safety Aspects and Toxicity of Hybrid Chitosan Gel

Figure 7 shows the results of the cytotoxicity analysis of the chitosan blend that hybridized the three different kinds of metal oxide nanoparticles with the cell lines A375 skin cell line (human malignant melanoma cell line) and WRL 68 cell line (the human hepatic cell line). Both cell lines were cultured in RPMI 1640 medium containing 10% (v/v) fetal calf serum, 100 U/mL penicillin and 100 µg/mL streptomycin at 37°C in a humidified 5% CO_2 incubator. Freshney's protocols [37] were followed while preparing the solutions and media for cell culture. For MTT assay: Using Intron Biotech's (Korea) MTT ready-to-use kit, the cytotoxic effect of the prepared sample was investigated. Tumor cells (5 × 104 cells/mL) were cultured in 96 flat well MTT, each well in a final volume of 200 mL of complete (RPMI) medium. For 24 hours, the plates were incubated at 37°C with 5% CO_2. Then, the culture medium was removed and serial dilutions of the gel (6.25, 12.5, 25, 50, 100, 200 and 400 mg/mL) were added to the wells.

The cell viability of the A375 cell line was measured using a multi-parameter cytotoxicity test after being exposed to varied concentrations of nanocomposite gel in vitro. The ArrayScan HCS analyzer was used to examine the plate (ThermoScientific). The HCS technique was carried out at the Centre

for Natural Product Research and Drug Discovery, University of Malaya, Kuala Lumpur, Malaysia. The data on viability rate for A375 cells treated by the gel are shown in Table 3. The results have indicated a considerable cytotoxicity and reduction of viability for A375 cell line along with the increase of the concentration, and the highest effect was at a concentration of 400 µg/mL.

The cytotoxic effects of chitosan embedded metal oxide nanopowders were measured in the WRL-68 by the MTT assay. WRL-68 cells were treated with varied doses of nanocomposite for 24 hours at 37°C. The rate of viability for WRL-68 treated with the gel is shown in Table 3. The results have revealed a slight reduction of cell viability for the compound on WRL-68, and the reduction in viability could be considered as stable at the safe range up to a concentration of 100 µg/mL. When comparing the two curves, one can notice that the value IC_{50} of cancer cells differs about 61% lower than the value IC_{50} for normal cell, this means that the prepared gel has toxic behavior for the cancer cell as compared to the normal cell. In other words, our product has high safety to be used with human tissue as a wound healer.

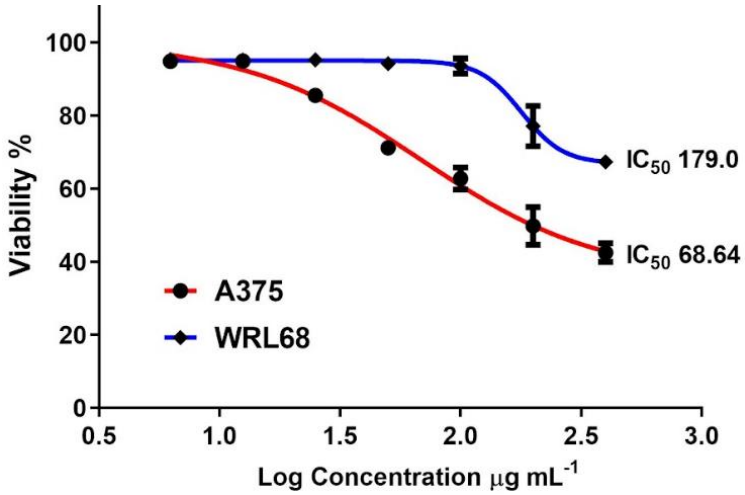

Figure 7. Dose-response curves of viability display the IC_{50} of nanohybrid chitosan effect on WRL-68 and A375 cell lines.

Table 3. Rate of viability for A375 and WRL-68 cells treated by the nanocomposite chitosan gel.

Concent. µg/ml	Log. Concent. µg/mL	A375		WRL68	
		Mean%	*±SD*	*Mean%*	*±SD*
400.00	2.6	42.52	2.57	67.32	1.97
200.00	2.3	49.81	5.21	77.08	5.52
100.00	2	62.73	3.07	93.60	2.10
50.00	1.6	71.14	0.82	94.17	1.57
25.00	1.4	85.53	1.80	95.22	0.82
12.50	1.1	94.87	0.29	95.18	0.41
6.25	0.8	94.83	0.71	95.29	1.05

Histological Analysis

Histological analysis was carried out to observe the changes in skin tissue during wound healing according to literature, especially for Luna procedure [38]. Figure 8 shows the healed tissues of injured mice after 7 days from the onset of the experiment that refers to the control sample (without treatment), cross-section of tissue treated by the effective gel (a ternary metal oxide group), the injured tissue that was treated by Fucidin cream labeled as a, b, and c, respectively, to the right side of the figure. The left side identifies the histological images of the previous explained tissues a, b, and c.

Histological findings at the wound site of the control group for a 7-day duration showed complete epithelialization and there was a decrease in number of inflammatory cells together with the formation of loose collagen fibers. Additionally, there was granulation tissue, which is characterized by the proliferation of endothelial cells along with the initiation of new blood vessels, as well as an irregular arrangement of collagen fibers, as shown in Figure 8a.

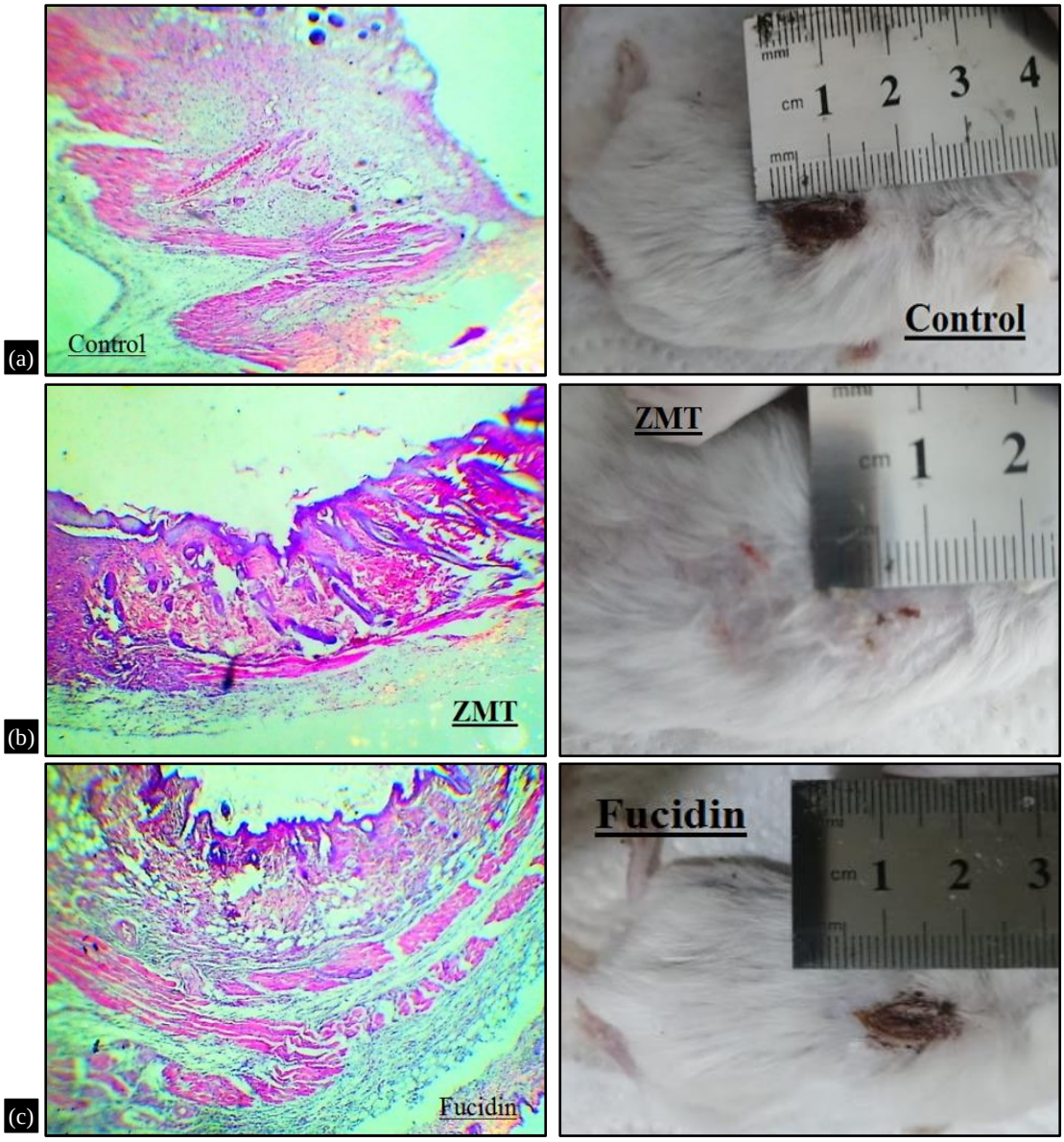

Figure 8. The histopathological studies of paraffin sections of biopsies of wounded areas after 7 days of the injury time. (The wound healing experiment showed that the combination of TiO_2, ZnO, MgO nanopowders with chitosan hydrogel significantly enhances healing of wounds in less than a week.) Left: Histological sections. Right: Healed mice tissues after a week from the start day of the experiment. (a) The control group: without treatment. (b) The treated group with the produced gel. (c) treated group by Fucidin cream.

The histological section at the wound site of treated wounds with ZMT gel for a 7-day duration revealed complete epithelialization, the new epithelium was thin with no rete-ridges, healed wound site with fibers, and the reduced cellular component can be detected. Furthermore, epithelial cell layers of the new epidermis and few fibroblasts are seen scattered throughout the fibers of the underlying dermis and formation of new blood vessels, as shown in Figure 8b.

Histological findings at the wound site of the Fucidin treated group for a 7-day duration exhibited complete epithelialization and there was a decrease in number of inflammatory cells together with the formation of loose collagen fibers, in addition to granulation tissue with the irregular arrangement of collagen fibers (Figure 8c).

CONCLUSION

Biodegradable blend gels composed of nano chitosan/PVA/PEG hybridized with various composition ratios of MgO, ZnO, and TiO_2 nanopowders were prepared. FTIR spectroscopy and FE-SEM microscopy were adopted to study their molecular interactions and surface morphology, respectively. DSC-TGA analysis was used to investigate thermal stability and degradation steps. In vivo and in vitro research were accomplished to examine the wound healing efficiency of the prepared hybrids as well as their toxicity on WRL-68 and A375 unit cells. CHT blend reinforced by typical ratios of MgO, ZnO, and TiO_2 collectively, has enhanced the blend property in wound healing. An in the vivo model revealed that the novel hybrid of CHT/PVA/PEG blend with the proposed metal oxides has superior efficiency than Fucidin ointment (medical product). The main evidence deduced at the end of this study is that wound contraction and reduction in the wound area were enhanced and achieved in less than a week According to the presence of notable markers of necrotic tissue, clotting and crust, re-epithelialization, and granulation tissue growth, chitosan blend and metal oxide nanoparticles have a significant efficiency in tissue repair. This is an indication of collagen maturation progress. Based on the results, our work puts forward a facile approach to synthesize a biodegradable, polymeric gel–based hybrid chitosan/tertiary nanometal oxides and paves the way for a new medical product for wound healing purposes.

Acknowledgement

We gratefully thank and appreciate the efforts of staff at the Department of Applied Sciences/the University of Technology-Iraq. The authors are responsible for their funding support.

Conflict of Interest

We (the authors) declare that we have no conflict of interest.

REFERENCES

1. Azimi B, Maleki H, Zavagna L, De la Ossa JG, Linari S, Lazzeri A, Danti S. Bio-based electrospun fibers for wound healing. J Funct Biomater. 2020; 11 (3): 67.
2. Reinke J, Sorg H. Wound repair and regeneration. Eur Surg Res. 2012; 49 (1): 35–43.
3. Abdulkareem M, Abdalsalam A, Bohan A. Influence of chitosan on the antibacterial activity of composite coating (PEEK/HAp) fabricated by electrophoretic deposition. Prog Org Coatings. 2019; 130: 251–259.
4. Reddy M, Ponnamma D, Choudhary R, Sadasivuni K. A comparative review of natural and synthetic biopolymer composite scaffolds. Polymers. 2021; 13 (7): 1105.
5. Al-Zubaydi ASJ, Salih RM, Al-Dabbagh BM. Effect of nano TiO_2 particles on the properties of carbon fiber-epoxy composites. Prog Rubber Plast Recycl Technol. 2021; 37 (3): 216–232.
6. Tudoroiu E, Dinu-Pîrvu C, Albu Kaya MG, Popa L, Anuța V, Prisada RM, Ghica MV. An overview of cellulose derivatives-based dressings for wound-healing management. Pharmaceuticals. 2021; 14 (12): 1215.
7. Rezvani Ghomi E, Khalili S, Nouri Khorasani S, Esmaeely Neisiany R, Ramakrishna S. Wound dressings: current advances and future directions. J Appl Polym Sci. 2019; 136 (27): 47738.
8. Sood A, Granick M, Tomaselli N. Wound dressings and comparative effectiveness data. Adv Wound Care. 2014; 3 (8): 511–529.
9. Nehia NH, Mina MK. Evaluation of the biosynthesized silver nanoparticles effects on biofilm formation. J Appl Sci Nanotechnol. 2021; 1 (1): 23–31.
10. Jawad A, Thewaini Q, Al-Musawi S. Cytotoxicity effect and antibacterial activity of Al_2O_3

nanoparticles activity against *Streptococcus pyogenes* and *Proteus vulgaris*. J Appl Sci Nanotechnol. 2021; 1 (3): 42–50.
11. Jabbar RA, Hussein NN. Evaluation the antibacterial activity of biosynthesis silver nanoparticles by *Lactobacillus gasseri* bacteria. J Appl Sci Nanotechnol. 2021; 1 (3): 86–95.
12. Fadhil IA. Investigation of USPION genotoxicity on cytokinesis blocked micronuclei. Int J Pharm Res. 2019; 11 (2): 115–120. doi: 10.31838/ijpr/2019.11.02.019.
13. Fadhil IA, Mohammed Dheyaa B, Thamir Mahdi W. Chitosan/PVA/PEG blend strengthened with MgO nanoparticles for antibacterial application. J Appl Sci Nanotechnol. 2022; 2 (3): 126–136. doi: 10.53293/jasn.2022.4552.1123.
14. Zheng H, Du Y, Yu J, Huang R, Zhang L. Preparation and characterization of chitosan/poly (vinyl alcohol) blend fibers. J Appl Polym Sci. 2001; 80 (13): 2558–2565.
15. Guan Y, Liu X, Zhang Y, Yao K. Study of phase behavior on chitosan/viscose rayon blend film. J Appl Polym Sci. 1998; 67 (12): 1965–1972.
16. Yin Y, Yao K, Cheng G, Ma J. Properties of polyelectrolyte complex films of chitosan and gelatin. Polym Int. 1999; 48 (6): 429–432.
17. Rocha-Santos T, Costa MF, Mouneyrac C. Handbook of Microplastics in the Environment. Cham, Switzerland: Springer; 2022.
18. Bukzem A, Signini R, dos Santos D, Lião L, Ascheri D. Optimization of carboxymethyl chitosan synthesis using response surface methodology and desirability function. Int J Biol Macromol. 2016; 85: 615–624.
19. Valencia-Gómez LE, Martel-Estrada SA, Vargas-Requena CL, Acevedo-Fernández JJ, Rodríguez-González CA, Hernández-Paz JF, Olivas-Armendáriz I. Characterization and evaluation of a novel O-carboxymethyl chitosan films with *Mimosa tenuiflora* extract for skin regeneration and wound healing. J Bioactive Compatible Polym. 2020; 35 (1): 39–56.
20. Mohandas A, Deepthi S, Biswas R, Jayakumar R. Chitosan based metallic nanocomposite scaffolds as antimicrobial wound dressings. Bioactive Mater. 2018; 3 (3): 267–2778.
21. Zainal Z, Hui LK, Hussein MZ, Abdullah AH, Hamadneh IR. Characterization of TiO_2–chitosan/glass photocatalyst for the removal of a monoazo dye via photodegradation–adsorption process. J Hazard Mater. 2009; 164 (1): 138–145.
22. Saravanan R, Aviles J, Gracia F, Mosquera E, Gupta VK. Crystallinity and lowering band gap induced visible light photocatalytic activity of TiO_2/CS (chitosan) nanocomposites. Int J Biol Macromol. 2018; 109: 1239–1245.
23. Farzana MH, Meenakshi S. Synergistic effect of chitosan and titanium dioxide on the removal of toxic dyes by the photodegradation technique. Indust Eng Chem Res. 2014; 53 (1): 55–63.
24. Raut AV, Yadav HM, Gnanamani A, Pushpavanam S, Pawar SH. Synthesis and characterization of chitosan-TiO_2:Cu nanocomposite and their enhanced antimicrobial activity with visible light. Colloids Surf B: Biointerfaces. 2016; 148: 566–575.
25. Anaya-Esparza L, Vargas-Torres A, Palma-Rodrigues HM, Castro-Mendoza MP, Yahia EM, Perez-Larios A, Montalvao-Gonzalez E. . Effect of mixed oxide-based TiO_2 on the physicochemical properties of chitosan films. Period Polytechn Chem Eng. 2022; 66 (3): 422–436.
26. Jayakumar R, Ramachandran R, Divyarani VV, Chennazhi KP, Tamura H, Nair SV. Fabrication of chitin–chitosan/nano TiO_2-composite scaffolds for tissue engineering applications. Int J Biol Macromol. 2011; 48 (2): 336–344.
27. Bispo V, Mansur A, Barbosa-Stancioli E, Mansur H. Biocompatibility of nanostructured chitosan/poly (vinyl alcohol) blends chemically crosslinked with genipin for biomedical applications. J Biomed Nanotechnol. 2010; 6 (2): 166–175.
28. Berger J, Reist M, Mayer JM, Felt O, Peppas NA, Gurny R. Structure and interactions in covalently and ionically crosslinked chitosan hydrogels for biomedical applications. Eur J Pharm Biopharm. 2004; 57 (1): 19–34.
29. Claper JD, Skeie JM, Mullins RF, Guymon CA. Development and characterization of

photopolymerizable biodegradable materials from PEG-PLA-PEG block macromonomers. Polymer. 2007; 48: 6554.
30. Gupta KC, Jabrail FH. Glutaraldehyde cross-linked chitosan microspheres for controlled release of centchroman. Carbohydr. Res. 2007; 342 (15): 2244–2252.
31. Zhang Y, Huang X, Duan B, Wu L, Li S, Yuan X. Preparation of electrospun chitosan/poly (vinyl alcohol) membranes. Colloid Polym Sci. 2007; 285: 855–863.
32. Salih AA, Nazar A, Haider AJ. Antibacterial activity of ZnO nanoparticle prepared by pulsed laser ablation in liquid for biological sensor. In: 2019 12th International Conference on Developments in eSystems Engineering (DeSE), Kazan, Russia, 2019, October 7–10. IEEE; 2019. pp. 726–729.
33. Zhang X, Liu Y, Yong H, Qin Y, Liu J, Liu J. Development of multifunctional food packaging films based on chitosan, TiO_2 nanoparticles and anthocyanin-rich black plum peel extract, Food Hydrocolloids. 2019; 94: 80–92.
34. Kavitha K, Sutha S, Prabhu M, Rajendran V, Jayakumar T. In situ synthesized novel biocompatible titania–chitosan nanocomposites with high surface area and antibacterial activity. Carbohydr Polym. 2013; 93 (2): 731–739.
35. Grande CD, Mangadlao J, Fan J, De Leon A, Delgado-Ospina J, Rojas JG, Rodrigues DF, Advincula R. Chitosan cross-linked graphene oxide nanocomposite films with antimicrobial activity for application in food industry. Macromol Symp. 2017; 374 (1): 1600114.
36. Jbeli A, Ferraria A, Botelho do Rego A, Boufi S, Bouattour S. Hybrid chitosan-TiO_2/ZnS prepared under mild conditions with visible-light driven photocatalytic activity. Int J Biol Macromol. 2018; 116: 1098–1104.
37. Capes-Davis A, Freshney RI. Freshney's Culture of Animal Cells: A Manual of Basic Technique and Specialized Applications. 8th edition. Hoboken, NJ: Wiley-Blackwell; 2021.
38. Kumbhalkar MA, Rangari DT, Pawar RD, Phadtare RA, Raut KR, Nagre AN. Finite element analysis of knee joint with special emphasis on patellar implant. In: Akinlabi ET, Ramkumar P, Selvaraj M, editors. Trends in Mechanical and Biomedical Design. Lecture Notes in Mechanical Engineering. Singapore: Springer; 2021. pp. 319–333. . doi: 10.1007/978-981-15-4488-0_29.

